Automated Detection of Welding Defects without Segmentation

Domingo Mery

Pontificia Universidad Catolica de Chile
Av. Vicuna Mackenna 4860(143), Santiago de Chile
dmery@ing.puc.cl
http://dmery.ing.puc.cl

Abstract
Substantial research has been performed on automated detection and classification of welding defects in continuous welds using X-ray imaging. Typically, the detection follows a pattern recognition schema (segmentation, feature extraction and classification). In computer vision community, however, many object detection and classification problems, like face and human detection, have been recently solved -without segmentation- using *sliding-windows* and novel features like local binary patterns extracted from saliency maps. For this reason, we propose in this paper the use of sliding-windows with the mentioned features to perform automatically the automated detection of welding defects. In the experiments, we analyzed 5000 detection windows (24x24 pixels) and 572 intensity features from 10 representative X-ray images. Cross validation yielded a detection performance of 94% using a support vector machine classifier with only 14 selected features. The method was implemented and tested on real X-ray images showing high effectiveness. We believe that the proposed approach opens new possibilities in the field of automated detection of welding defects.

1. INTRODUCTION

In the last three decades, substantial research has been performed on automated detection and classification of welding defects in continuous welds using X-ray imaging (Silva and Mery, 2007a; Silva and Mery 2007b). Typically, the approaches follow a classical pattern recognition schema: *i)* image acquisition -an X-ray digital image is taken and stored in the computer, *ii)* pre-processing -the digital image is improved in order to enhance the details, *iii)* segmentation -potential welding defects are found and isolated, *iv)* feature extraction/selection -significant features of the potential welding defects and their surroundings are quantified, and *v)* classification -the extracted features are interpreted automatically using a priori knowledge of the welding defects in order to separate potential welding defects into detected welding defects or false alarms.

In computer vision community, however, many object detection and classification problems have been recently solved -without segmentation- using s*liding-windows*. Sliding-window approaches have established themselves as state-of-the-art in computer vision problems where an object must be separated from the background (see for example successful applications in face detection (Viola and Jones, 2004) and human detection (Dalal and Triggs, 2005). In sliding-window methodology, a detection window (see black square in Fig. 1) is sledded over an input image in both horizontal and vertical directions, and for each localization of the detection window, a

classifier decides to which class belongs the corresponding portion of the image according to its features. In this step, novel features developed in the last years like *local binary patterns* (texture information extracted from occurrence histogram (Ojala et al., 2002)) and *saliency maps* (an image transformation based on a biologically inspired attention system (Montabone and Soto, 2010)) can be used to describe the detection windows in a better way.

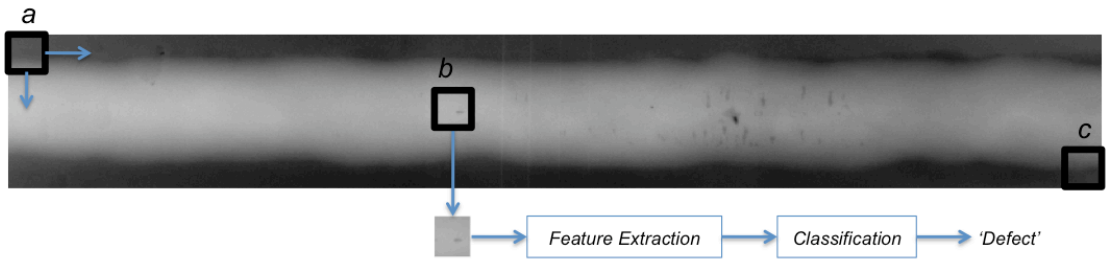

Fig. 1: Sliding-window approach: A detection window (see black square) is sledded over the X-ray image starting at place 'a' and ending at 'c'. For each position, *e.g.* at 'b', features are extracted only from the detection window defined by the square, and a classifier determines the class of this portion of the image.

To the best of our knowledge, there is no approach to detect welding defects that use this novel computer vision methodology (see a literature review until 2007 in (Silva and Mery, 2007a; Silva and Mery 2007b) and more recent articles in (Shi et al, 2007; Liao, 2008; Liao, 2009)). For this reason, we developed and tested an X-ray computer vision approach to detect welding defects based on this methodology. We differentiate between the *detection* of defects and the *classification* of defects (Liao, 2003). In the detection problem, the classes that exist are only two: 'defects' and 'no-defects', whereas the recognition of the type of the defects (e.g., porosity, slag, crack, lack of penetration, etc.) is known as classification of flaws types. This paper describes our approach on detection only and the corresponding validation experiments. The classification of defects using a similar methodology will be tested in the next future.

The rest of the paper is organized as follows: In Section 2, the proposed X-ray computer vision approach is explained. In Section 3, the results obtained in several experiments on X-ray images are shown. Finally, in Section 4 some concluding remarks are given.

2. COMPUTER VISION

The key idea of our work is to use a computer vision methodology, as shown in Fig. 1 and Fig. 2, to automatically detect welding defects. In following, feature extraction, feature selection, detection and validation will be explained in further detail.

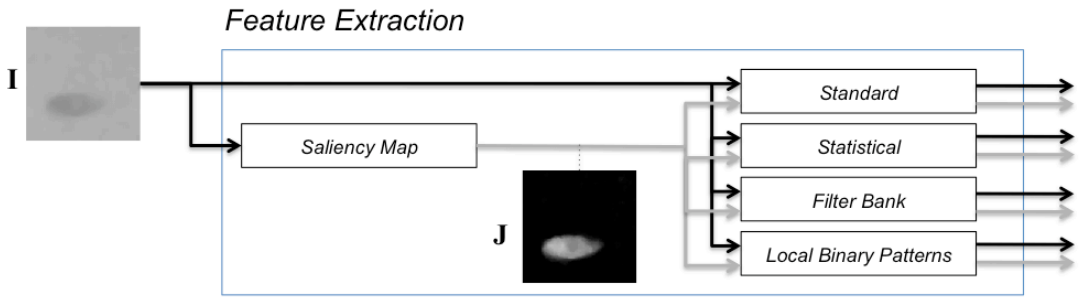

Figure 2: Feature extraction: from each detection window **I** several features are extracted (see black path). Additionally, the same features are extracted from a saliency map **J** of the detection window (see gray path).

2.1 FEATURE EXTRACTION

Features provides information about the intensity of a detection window. In our approach, *p* features per *intensity* channel were extracted. The used intensity channels in our work are only two: the grayscale X-ray image **I** and a saliency map **J** computed from **I**, *i.e.*, *p* x 2 features for two intensity channels. In order to reduce the computational time, we restricted the feature extraction for these only two channels, however, other channels, like Harris transform (Harris and Stephens, 1988) or other saliency maps, can be used (Montabone and Soto, 2010).

The saliency map **J** is obtained using a center-surround saliency mechanism based on a biologically inspired attention system (Montabone and Soto, 2010). In order to achieve faster processing, this theory proposes that the human visual system uses only a portion of the image, called *focus of attention*, to deal with complex scenes. In our approach we use the *off-center* saliency map that measures the different of dark areas surrounded by a bright background, as shown in Fig. 2.

In a training phase, using a priori knowledge of the welding defects, the detection windows are manually labeled as one of two classes: *defects* and *no-defect*. The first class corresponds to real welding defects. Alternatively, the second class corresponds to false alarms. Intensity features of each channel are extracted for both classes. Features extracted from each area of an X-ray image region are divided into four groups as shown in Table 1. The following four groups of features were used for each intensity channel.

1. Standard: Simple intensity information related to the mean, standard deviation of the intensity in the region, mean first derivative in the boundary, and second derivative in the region (Nixon and Aguado, 2008).

2. Statistical textures: Texture information extracted from the distribution of the intensity values based on the Haralick approach (Haralick, 1979). They are computed utilizing *co-occurrence matrices* that represent second order texture information (the joint probability distribution of intensity pairs of neighboring pixels in the image), where mean and range of the following variables were measured: Angular Second Moment, Contrast, Correlation, Sum of squares, Inverse Difference Moment, Sum Average, Sum Entropy, Sum Variance, Entropy, Difference Variance, Difference Entropy, Information Measures of Correlation, and Maximal Correlation Coefficient.

Table 1: Extracted Features

Group		Name and references
1	Standard	Mean Intensity, Standard deviation Intensity, Mean Laplacian, Mean Gradient, etc. (Nixon and Aguado, 2008).
2	Statistical Textures	Tx(k,p) (mean/range) for k=1. Angular Second Moment 2. Contrast, Correlation, 4. Sum of squares, 5. Inverse Difference Moment, 6. Sum Average, 7. Sum Entropy, 8. Sum Variance, 9. Entropy, 10. Difference Variance, 11. Difference Entropy, 12.,13. Information Measures of Correlation, 14. Maximal Correlation Coefficient, and p=1,...5 pixels (Haralick, 1979).
3	Filter Banks	DFT (1,2;1,2) and DCT (1,2;1,2) (Gonzalez and Woods, 2008). Gabor (1,...,8;1,...8), max(Gabor), min(Gabor), Gabor-J (Kumar and Pang, 2002).
4	Local Binary Patterns	LBP(1,…,59) (Ojala et al., 2002).

3. Filter banks: Texture information extracted from image transformations like Discrete Fourier Transform (DFT), Discrete Cosine Transform (DCT) (Gonzalez and Woods, 2008), and Gabor features based on 2D Gabor functions, *i.e.*, Gaussian-shaped bandpass filters, with dyadic treatment of the radial spatial frequency range and multiple orientations, which represent an appropriate choice for tasks requiring simultaneous measurement in both space and frequency domains, usually 8 scale and 8 orientations (Kumar and Pang, 2002).

4. Local binary patterns: Texture information extracted from occurrence histogram of *local binary patterns* (LBP) computed from the relationship between each pixel intensity value with its eight neighbors. The features are the frequencies of each one of the histogram's 59 bins. LBP is very robust in terms of gray-scale and rotation variations (Ojala et al., 2002).

In our experiments, p=286 features are extracted from each detection window and for each channel, *i.e.*, n=286 x 2 =572 features in total.

2.2 FEATURE SELECTION

The extracted features must be selected in order to decide on the relevant features for the two defined classes.

The n extracted features for sample i are arranged in an n-vector: $\mathbf{f}_i = [f_{i1} \ldots f_{in}]$ that corresponds to a point in the n-dimensional measurement feature space. The features are normalized yielding a N x n matrix **W** which elements are defined as:

$$w_{ij} = \frac{f_{ij} - \mu_j}{\sigma_j} \quad (1)$$

for i=1,...,N and j=1,...,n, where f_{ij} denotes the j-th feature of the i-th feature vector, N is the number of samples and μ_j and σ_j are the mean and standard deviation of the j-th feature. Thus, the normalized features have zero mean and a standard deviation equal to one. Those high correlated features can be eliminated because they do not provide relevant information about the welding defects.

In feature selection, a subset of m features ($m<n$) that leads to the smallest detection error is selected. The selected m features are arranged in a new m-vector $\mathbf{s}_i = [s_{i1} \ldots s_{im}]^T$. This can be understood as a matrix $\mathbf{S}$ with N x m elements obtained from m selected columns of the large set of normalized features $\mathbf{W}$.

The features can be selected using several state-of-art algorithms documented in literature like Forward Orthogonal Search (Wei and Billings, 2007), Least Square Estimation (Mao, 2005), Ranking by Class Separability Criteria (MathWorks, 2007) and Combination with Principal Components (Bishop, 2006) among others. However, in our experiments the best performance was achieved using the well-known Sequential Forward Selection (SFS) algorithm (Jain et al., 2000). This method selects the best single feature and then adds one feature at a time that, in combination with the selected features, maximizes detection performance. The iteration is halted once no considerable improvement in the performance is achieved by adding a new feature. By evaluating selection performance we ensure: *i)* a small intraclass variation and *ii)* a large interclass variation in the space of the selected features. For the first and second conditions the intraclass-covariance $\mathbf{C}_b$ and interclass-covariance $\mathbf{C}_w$ of the selected features $\mathbf{S}$ are used respectively. Selection performance can be evaluated using:

$$J(\mathbf{S}) = \mathrm{trace}(\mathbf{C}_w^{-1}\mathbf{C}_b) \qquad (2)$$

where `trace' means the sum of the diagonal elements. The larger the objective function J, the higher the selection performance.

The implementation of SFS is simple: one starts with an empty matrix $\mathbf{S}_o$ for the selected features and a list $L = \{ 1, 2, 3, \ldots n \}$ containing the index of all available features. The following iteration is performed: *i*) the feature $j \in L$ is selected using exhaustive search so that equation (2) is maximized for $\mathbf{S} = [\mathbf{S}_o \ \mathbf{w}_j]$, where $\mathbf{w}_j$ is the j-th column of $\mathbf{W}$; *ii*) j is eliminated from L, and *iii*) the selected features matrix $\mathbf{S}_o$ is replaced by $\mathbf{S}$. This iteration is repeated $m<n$ times or until no significant improvement in J is achieved.

2.3 DETECTION

A classifier decides whether the detection windows are *defects* or *no-defects*. The detection in this case is a classification with only two classes. In order to find the best detection performance, the framework was tested on a bank of classifiers, such as support vector machines (SVM) (Shawe-Taylor and Cristianini, 2004), linear and quadratic discriminant analysis (LDA and QDA) (Webb, 2005), k-nearest neighbor (KNN) (Duda and Hart, 2001), neural networks (Bishop, 2006), boosting (Viola and Jone, 2004) and minimal and Mahalanobis distances (Duda and Hart, 2001). The best performance was achieved using SVM. SVM transforms a two-class feature space, defined by feature vector $\mathbf{s}$ of dimension m, where the two classes overlap, into a new enlarged feature space, defined by transformation $h(\mathbf{s})$, where the classification boundary is linear. Thus, a simple linear classifier can be designed in the transformed feature space in order to separate both classes. For the detection decision of a sample $\mathbf{s'}$, however, only the kernel function $K(\mathbf{s},\mathbf{s'}) = < h(\mathbf{s}), h(\mathbf{s'}) >$ that computes inner products in the transformed space is required (see (Shawe-Taylor and Cristianini, 2004) for details). In our case, the best classification was obtained using a *Gaussian Radial Basis* (RBF) function kernel defined by:

$$K(\mathbf{s},\mathbf{s}') = e^{\|s-s'\|^2} \quad (3)$$

where the linear boundary, *i.e.*, the separating hyperplane in the transformed space, is computed using the Least-Squares approach (MathWorks, 2007).

2.4 VALIDATION

The performance of the detection was defined as the ratio of the detection windows that were correctly classified to the total number of detection windows. The performance was validated using cross-validation, a technique widely implemented in machine learning problems (Mithcell, 1997). In cross-validation, the samples are divided into F folds randomly. F-1 folds are used as training data and the remaining fold is used as testing data to evaluate the performance of the classifiers. We repeated this experiment F times rotating train and test data. The F individual performances from the folds are averaged to estimate the final performance of the classifiers.

3. EXPERIMENTAL RESULTS

We experimented with 10 representative X-ray images (see Fig. 3)[1]. The average size of the images were 1.35 mega-pixels. For each X-ray image, 250 detection windows with defects and 250 without defects were selected, yielding 2x250x10 = 5000 detection windows. Each detection window was labeled with '1' for class *defects* and '0' for *no-defects*. We tested for different sizes (8x8, 16x16, 24x24 and 32x32 pixels), the best performance was achieved by using 24x24 pixels. For each detection window 572 features were extracted according to Section 2.1. This means that 572 features were extracted from 5000 samples (2500 with defects and 2500 without defects).

After the feature extraction, 75% of the samples from each class were randomly chosen to perform the feature selection. The best performance was achieved using Sequential Forward Selection. The SFS iteration was stopped by m=14, because for m >14 no significant improvement (<2%) in objective function J (see equation (2)) was obtained.

The performance of the classification using SVM-RBF classifier and the first m selected features was validated using an average of ten cross-validation with F=10 folds[2] as explained in Section 2.4. The results are shown in Fig 4. For example using the first 8 selected features a detection performance of 90% was achieved. We observed that for m >14 no significant better performance could be obtained. Using the best 14 features, the performance was 93.74% with a 95% confidence interval between 92.97 and 94.51%. We observe the relevance of the saliency map features (10 of 14 features) and the local binary pattern features (9 of 14 features).

---

[1] All feature extraction, feature selection, classification and validation approaches are implemented in *Balu Matlab Toolbox* - Group of Machine Intelligence, Department of Computer Science, Catholic University of Chile (download in http://dmery.ing.puc.cl).

[2] F can be another number, for instance 5-fold or 20-fold cross-validation estimate very similar performances. In our experiments, we use 10-fold cross-validation because it has become the standard method in practical terms (Witten and Frank, 2005).

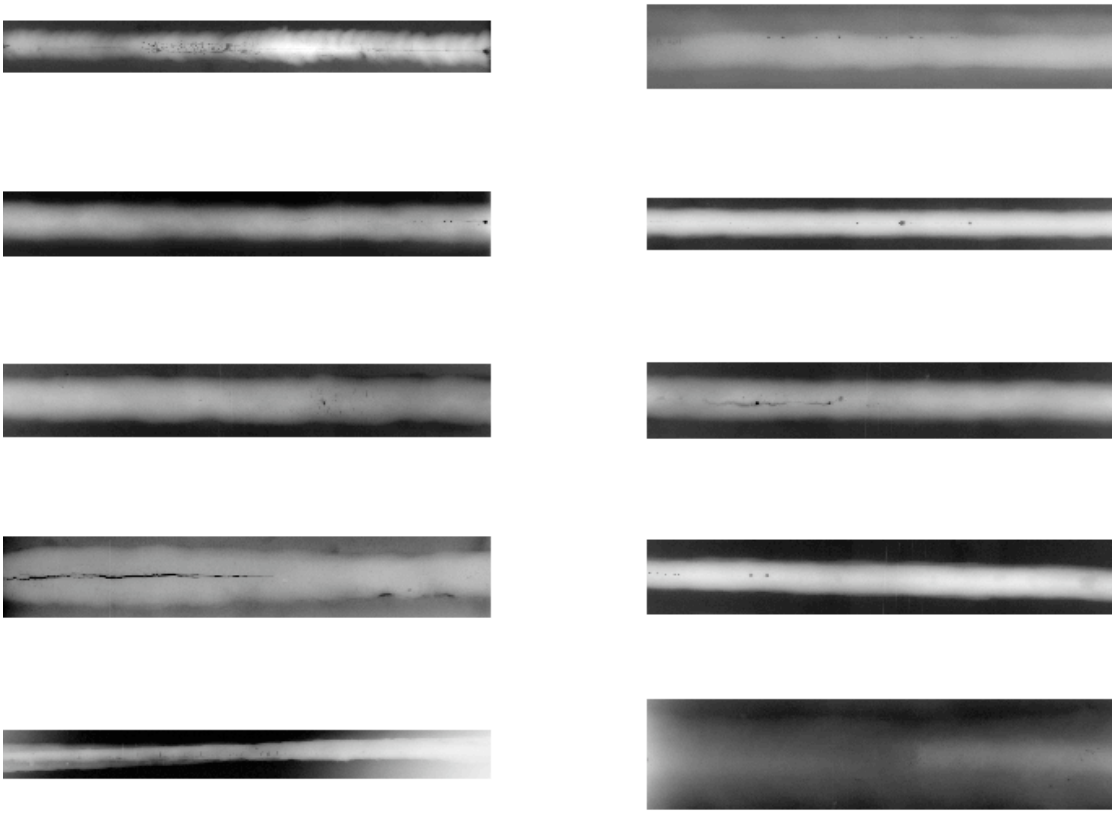

Fig. 3: X-ray images used in our experiments -courtesy of Federal Institute for Materials Research and Testing, Berlin (BAM).

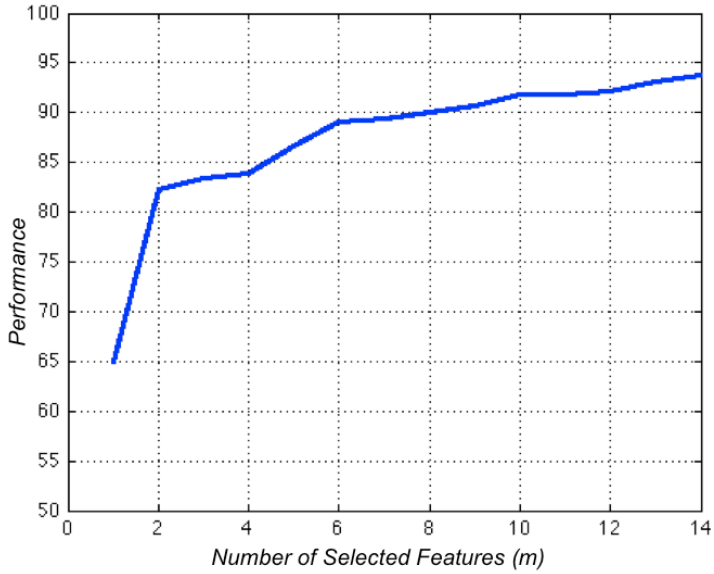

m	Name	Channel
1	LBP(36)	*Saliency*
2	LBP(1)	*Saliency*
3	LBP(13)	*Saliency*
4	Int-Hu-Moment(1)	*Saliency*
5	LBP(32)	*Saliency*
6	Tx12,d1(range)	*Saliency*
7	Tx14,d2(range)	*Saliency*
8	LBP(58)	*Saliency*
9	LBP(54)	*Saliency*
10	LBP(42)	*Gray*
11	Tx 1,d1(mean)	*Saliency*
12	LBP(14)	*Gray*
13	Fourier(1,1)	*Gray*
14	LBP(4)	*Gray*

Selected Features

Fig. 4: Classification performance with SVM-RBF using the first *m* features (refer to Table 1 to see a description of the features).

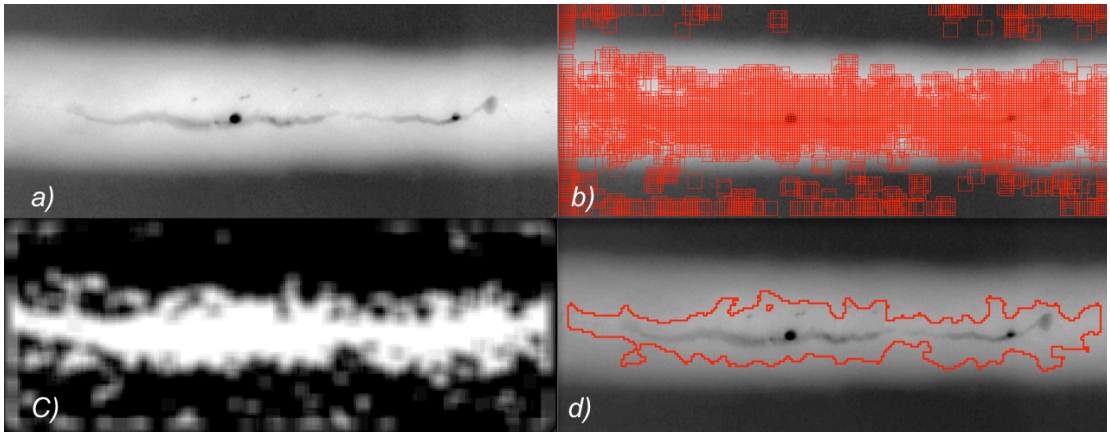

Fig. 5: Steps of the detection: a) original X-ray image, b) detected subwindows, c) grayvalue image that shows the number of detected subwindows per pixels (black=0, white=36), and d) final detection obtained by thresholding image c).

In order to test this method on X-ray images, the method was implemented using a sliding window sized 24x24 pixels that was shifted by 4 pixels. Thus, in each position a subwindow of 24x24 pixels was defined and the corresponding features were extracted. The subwindow was marked if the trained classifier detected it as a 'defect'. Using a size of 24x24 pixel and a shift of 4 pixels an image pixel could be marked 0, 1, 2, 3, … or 36 times. Finally, if a pixel of the image was marked more than 24 times, then the pixel was considered as defect. The mentioned parameters were set using exhaustive search. The described steps are shown in Fig. 5 for one X-ray image. The results on other X-ray images are shown in Fig. 6. We can see the effectiveness of the proposed method.

4. CONCLUSIONS

In this paper we presented a new approach to detecting weld defects without segmentation based on sliding-windows and novel features. The promising results outlined in our work show that we achieved a very high classification rate in the detection of welding defects using a large number of features combined with efficient feature selection and classification algorithms. The key idea of the proposed method was to select, from a large universe of features, namely 572 features, only those features that were relevant for the separation of the two classes. We tested our method on 10 representative X-ray images yielding a performance of 94% in accuracy using only 14 features and support vector machines. It is important to note that local binary pattern features extracted from the saliency map play an important role in the performance of the classifier. The method was implemented and tested on real X-ray images showing high effectiveness.

ACKNOWLEDGMENT

The radiographic material used in this investigation was given by the Federal Institute for Materials Research and Testing, Berlin (BAM). I thank Alvaro Soto, Sebastian Montabone and Christian Pieringer for discussion and developing the code of saliency maps. This work was supported by Fondecyt Project Number 1100830.

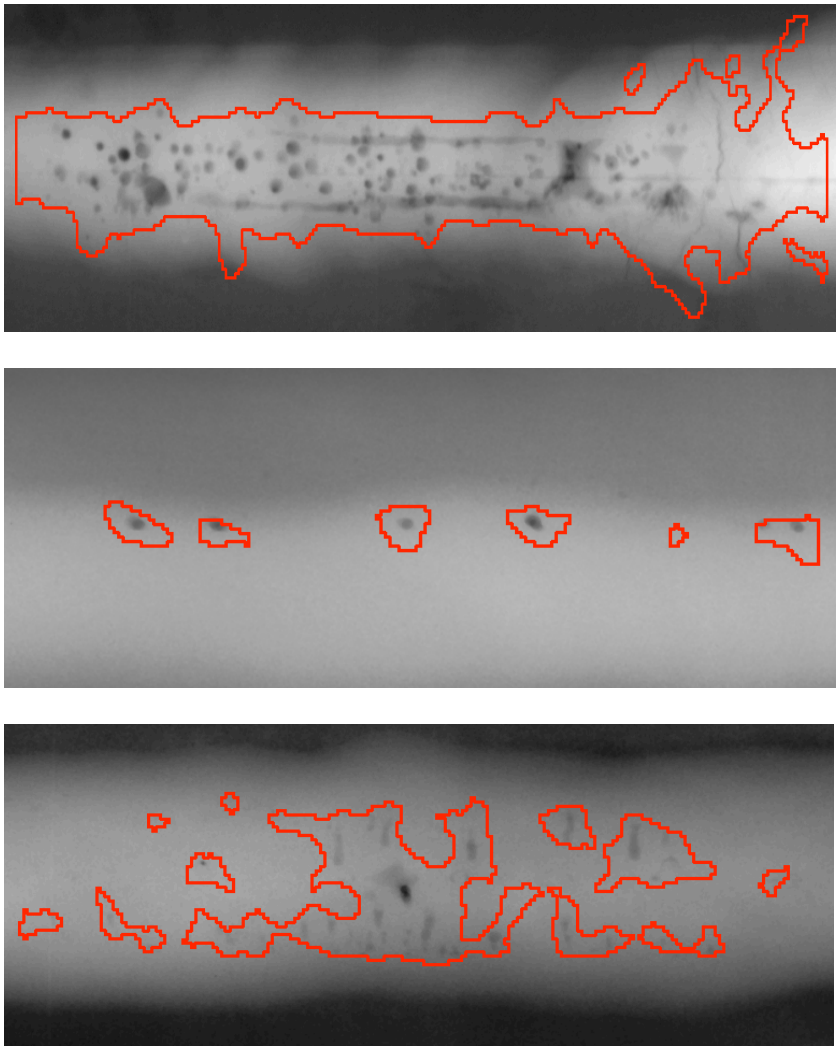

Fig. 6: Detection on X-ray images.

REFERENCES

Bishop, C.M. “Pattern Recognition and Machine Learning”. Springer, 2006.

Dalal, N. and Triggs, B. “Histograms of oriented gradients for human detection”. In Proceedings of the Conference on Computer Vision and Pattern Recognition (CVPR2005), Vol. 1, p. 886–893, 2005.

Duda, R.O., Hart, P.E. and Stork, D.G. “Pattern Classification”. John Wiley & Sons, Inc., New York, 2 edition, 2001.

Gonzalez, R.C. and Woods, R.E. “Digital Image Processing”. Pearson, Prentice Hall, third edition, 2008.

Haralick, R.M. “Statistical and structural approaches to texture”. Proc. IEEE, Vol. 67, No. 5, p. 786–804, 1979.

Harris, C. and Stephens, M.J. “A combined corner and edge detector”. In Proceedings of 4th Alvey Vision Conferences, p.147–152, 1988.

Hastie, T., Tibshirani, R. and Friedman, J. “The Elements of Statistical Learning: Data Mining, Inference, and Prediction”. Springer, corrected edition, August 2003.

Jain, A.K., Duin, R.P.W. and Mao, J. “Statistical pattern recognition: A review”. IEEE Trans. On Pattern Analysis and Machine Intelligence, Vol. 22, No. 1, p. 4–37, 2000.

Kumar, A. and Pang, G.K.H. “Defect detection in textured materials using Gabor filters”. IEEE Trans. on Industry Applications, Vol. 38, No. 2, p. 425–440, 2002.

Liao, T.W. “Classification of weld flaws with imbalanced class data”. Expert Systems with Applications, Vol. 35, No. 3, p. 1041–1052, 2008.

Liao, T.W. “Classification of welding flaw types with fuzzy expert systems”. Fuzzy Sets and Systems, Vol. 108, p. 145–158, 2003.

Liao, T.W. “Improving the accuracy of computer-aided radiographic weld inspection by feature selection”. NDT&E International, Vol. 42, p. 229–239, 2009.

Mao, K.Z. “Identifying critical variables of principal components for unsupervised feature selection”. IEEE Trans. on Systems, Man, and Cybernetics, Part B: Cybernetics, Vol. 35, No. 2, p. 339–344, 2005.

MathWorks. “Matlab Toolbox of Bioinformatics: User’s Guide”. Mathworks Inc., 2007.

Mitchell, T.M. “Machine Learning”. McGraw-Hill, Boston, 1997.

Montabone, S. and Soto, A. “Human detection using a mobile platform and novel features derived from a visual saliency mechanism”. Image and Vision Computing, Vol. 28, No. 3, p. 391–402, 2010.

Nixon, M. and Aguado, A. “Feature Extraction and Image Processing”. Academic Press, second edition, 2008.

Ojala, T, Pietikainen, M. and Maenpaa, T. “Multiresolution gray-scale and rotation invariant texture classification with local binary patterns”. IEEE Trans. on Pattern Analysis and Machine Intelligence, Vol. 24, No. 7, p. 971–987, 2002.

Shawe-Taylor J., and Cristianini. N. “Kernel Methods for Pattern Analysis”. Cambridge University Press, 2004.

Shi, D.-H., Gang, T., Yang, S.Y., and Yuan, Y. “Research on segmentation and distribution features of small defects in precision weldments with complex structure”. NDT & E International, Vol. 40, p. 397–404, 2007.

Silva, R. and Mery, D. “State-of-the-art of weld seam inspection using X-ray testing: Part I -Image Processing”. Materials Evaluation, Vol. 65, No 6, p. 643–647, 2007.

Silva, R. and Mery, D. “State-of-the-art of weld seam inspection using X-ray testing: Part II - Pattern Recognition”. Materials Evaluation, Vol. 65, No. 9, p. 833–838, 2007.

Viola, P. and Jones, M. “Robust real-time object detection”. International Journal of Computer Vision, Vol. 57, No. 2, p. 137–154, 2004.

Webb, A. “Statistical Pattern Recognition”. Wiley, England, 2005.

Wei, H.-L. and Billings, S.A. “Feature subset selection and ranking for data dimensionality reduction”. IEEE Trans. On Pattern Analysis and Machine Intelligence, Vol. 29, No. 1, p. 162–166, 2007.

Witten, I.H. and Frank, E. “Data Mining: Practical Learning Tools and Techniques”, Elsevier, Morgan Kaufmann Publishers, second edition, 2005.